Organic & Biomolecular Chemistry

ROYAL SOCIETY OF CHEMISTRY

COMMUNICATION

View Article Online
View Journal | View Issue

Cite this: *Org. Biomol. Chem.*, 2025, **23**, 4360

Received 11th February 2025,
Accepted 3rd April 2025

DOI: 10.1039/d5ob00245a

rsc.li/obc

Electron-deficient hemicryptophanes for the recognition of anions through anion–π interactions†

Louise Miton, [a] Pierre-Antoine Dupin, [a] Elise Antonetti, [a] Marion Jean,[b] Paola Nava, [a] Alexandre Martinez *[a] and Yoann Cotelle *[a]

The selective recognition and encapsulation of anions are crucial in many biological and environmental processes. Anion–π interactions, characterized by attractive non-covalent interactions between anions and electron-deficient aromatic surfaces, have gained significant attention for their potential in anion binding. However, due to the weak nature of these interactions, receptors that rely solely on anion–π interactions are scarce. To promote anion binding *via* electron-deficient surfaces, we constructed a cavity within the hemicryptophane framework using tetrafluoroxylylene arms and a benzene triimide unit, thereby displaying multiple electron-deficient surfaces. Binding studies revealed that the electron-deficient receptor exhibits significantly higher anion binding constants compared to a less electron-deficient hemicryptophane. For example, the affinity for chloride (K_a = 207) is ten times higher for the most electron-deficient hemicryptophane. More impressive is the unique affinity for triiodide (K_a = 416), representing the first example of triiodide recognition by a BTI-based receptor. The enhanced binding properties of this receptor result from the combination of different π-acidic surfaces in a single cage molecule.

Introduction

Anions are involved in many biological and environmental processes, making their selective recognition and encapsulation highly interesting.[1–5] Among others, the anion–π interaction has recently emerged as a promising mode of interaction.[6–10] Nonetheless, only a limited number of receptors able to bind anions solely through anion–π interactions have been reported.[11–16] Anion–π interactions are defined as attractive non-covalent interactions between an electron-deficient aromatic surface with a positive quadrupolar moment (Q_{ZZ}) and an anion.[17] In order to increase the strength of this interaction, we aim to explore the synergy of several π-acidic aromatic surfaces within a hemicryptophane to create a well-defined electron-deficient confined space.[18] Hemicryptophanes are composed of a preorganizing cyclotriveratrylene unit covalently linked to another unit having a C_3 symmetry axis.[19] To maximize interactions with anions, our attention turned towards the use of benzene triimides (BTIs),[20–22] which possess a high quadrupolar moment (Q_{ZZ} = 17.2 B, computed at the MP2/aug-cc-pVTZ level) and a suitable geometry. BTIs have recently been used in the design of molecular cages by bridging two BTI units with three *meta*-xylylene linkers, showing strong affinity and selectivity for azide.[23] Moreover, increasing the length of the spacers using naphthalene units has an impact on the selectivity for anions with different geometries.[24] We have recently described the synthesis of the BTI-based hemicryptophane **2** with xylylene linkers, showing promising lone pair–π interactions in the solid state.[25] Consequently, we introduced additional electron-withdrawing groups on the linkers to increase the binding for anions. Herein, we report the synthesis and characterization of an electron-deficient hemicryptophane and its increased anion binding ability compared to the hemicryptophane lacking additional electron-deficient linkers (Fig. 1).

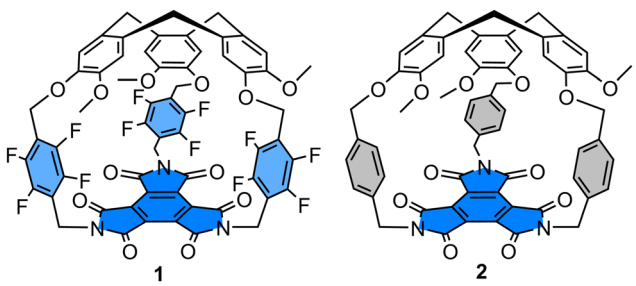

Fig. 1 Structure of the electron-deficient hemicryptophane **1** and the parent hemicryptophane **2** lacking electron-deficient linkers.

[a]*Aix Marseille Univ, CNRS, Centrale Med, ISM2, Marseille, France.*
E-mail: alexandre.martinez@centrale-marseille.fr, yoann.cotelle@univ-amu.fr
[b]*Aix Marseille Université, CNRS, FSCM, Chiropole, F-13397 Marseille, France*

† Electronic supplementary information (ESI) available. See DOI: https://doi.org/10.1039/d5ob00245a

Results and discussion

Hemicryptophane **1** was synthesized in three steps from the vanillyl alcohol precursor **3**. The first step involved the mono-alkylation of precursor **3** using an excess of bis(bromomethyl)-2,3,5,6-tetrafluorobenzene reagent and K_2CO_3 in acetone, resulting in compound **4** with a reasonable yield (49%). Then, the formation of the cyclotriveratrylene (CTV) unit was achieved through a triple Friedel–Crafts reaction, catalyzed by $Sc(OTf)_3$ in acetonitrile, giving the desired product **5** with a moderate yield (36%). Finally, a nucleophilic substitution on precursor **5** using BTI and DIPEA in DMF gave hemicryptophane **1** (38% yield) (Scheme 1).

The final compound was fully characterized by ^{1}H NMR, ^{13}C NMR and MS techniques (see ESI†). The ^{1}H NMR spectrum of receptor **1** is consistent with C_3 symmetry in solution (Fig. 2). Protons H_e and H_a are observed as doublets at 3.52 and 4.73 ppm, respectively. Methoxy protons appear as a singlet at 3.74 ppm, while the methylene bridges of the tetrafluoroparaxylylene spacers appear as doublets at 4.88 and 5.21 ppm for protons H_3 and at 5.26 and 5.53 for protons H_4. Finally, the aromatic protons of the CTV unit appear as singlets at 6.81 and 7.14 ppm for H_1 and H_2.

It was previously demonstrated that hemicryptophane **2** is a solvent-dependent chiral molecular switch, with an open CTV configuration in common organic solvents (including chloroform) and an inverted configuration in bulky polar aromatic solvents (such as 2-*t*-butylphenol).[25] Thus, we evaluated the configurational stability of hemicryptophane **1**. The racemic mixture of hemicryptophane **1** was resolved by chiral stationary phase HPLC on analytical and semi-preparative scales using a Chiralpak IA stationary phase and an ethanol/dichloromethane mixture (40/60) as the eluent (Fig. 3a). Contrary to the chromatogram of hemicryptophane **2**, we could observe only two peaks in the chromatogram of hemicryptophane **1**. Hence, no inverted configuration was observed in the chromatogram of cage **1**. This behavior strongly differs from that of cage **2**, which gives a mixture of in and out configurations under similar conditions, supporting the higher configurational stability of cage **1** compared to cage **2**. Subsequently, ECD spectra were recorded (Fig. 3b). The ECD spectra show two mirror images typical of the open configuration, confirming their enantiomeric nature. The absolute configuration of each enantiomer can be assigned by referring to the work of André Collet and Giovanni Gottarelli published in 1985.[26] Their study on cyclotriveratrylenes demonstrated that the absolute configuration of a CTV moiety could be determined by analyzing the sign changes of bands in the ECD spectrum, particularly at the ^1L_a transition (around 240 nm), as this transition was less sensitive to the substituents on the CTV. Thus, based on the ECD spectrum of hemicryptophane **1**, we propose that the first eluted enantiomer (green spectrum) is associated with the stereodescriptor *M*, while the second eluted enantiomer (red spectrum) is linked to the stereodescriptor *P*.

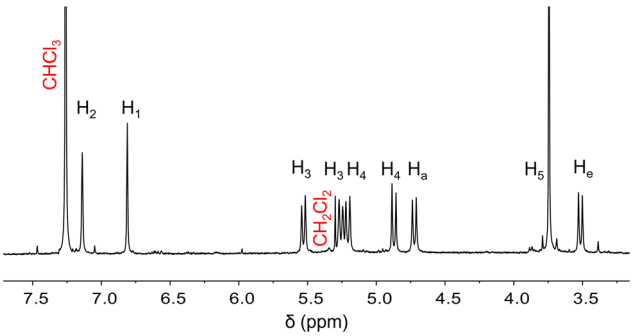

Fig. 2 ^{1}H NMR of hemicryptophane **1** ($CDCl_3$, 400 MHz, 298 K).

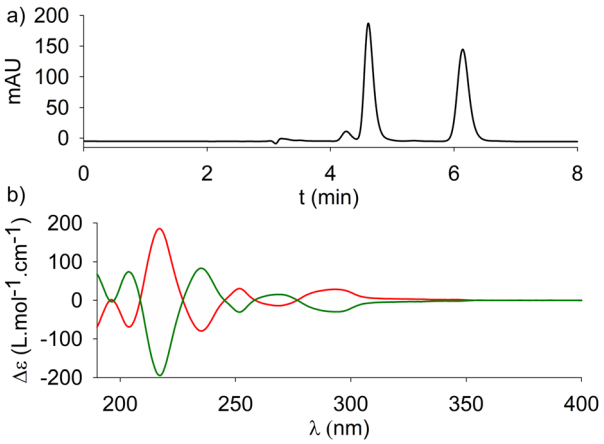

Fig. 3 (a) Analytical chiral HPLC chromatogram. (b) ECD spectra of the first eluted compound (*M*)-**1** (in green, c = 0, 140 mmol L^{-1}, CH_3CN) and the second eluted (*P*)-**1** (in red, c = 0.125 mmol L^{-1}, CH_3CN).

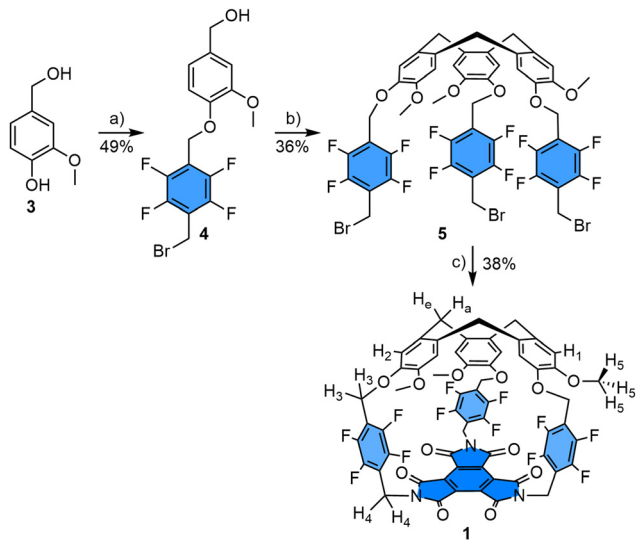

Scheme 1 Synthesis of hemicryptophane **1**. Conditions: (a) 1,4-bis(bromomethyl)-2,3,5,6-tetrafluorobenzene, K_2CO_3, acetone, 70 °C, 18 h. (b) $Sc(OTf)_3$, CH_3CN, 65 °C, 48 h. (c) BTI, DIPEA, DMF, 60 °C, 72 h.

Next, DFT calculations were performed to propose a structure as well as to determine the volume and ESP (electrostatic potential) maps of hemicryptophanes **1** and **2**. Hemicryptophane **1** was optimized as a C_3 symmetric object, in agreement with the ^{1}H NMR spectrum (Fig. 2), and has a large cavity (V = 327 Å^3), comparable to that of hemicryptophane **2** (V = 310 Å^3). Thus, both cages have a very similar shape and inner volume, and the change in binding affinity should arise from their differences in electron distribution. The ESP maps depict a strong difference in electron distribution between the two receptors. Hemicryptophane **1** with tetrafluoroxylylene linkers has more electron-deficient aromatic spacers, which should increase the binding for anionic species through anion–π interactions (Fig. 4c).

Finally, the recognition of anions by hemicryptophanes **1** and **2** was investigated. ^{1}H NMR titrations were performed in $CDCl_3$ by adding aliquots of tetrabutylammonium salts, to avoid inclusion of the counter ion, to a solution of the host.[27] All the constants were obtained by plotting the chemical shifts of the methylenic protons (H_4) of the linkers and fitting the data using a 1 : 1 stoichiometry with the BindFit program.[28] Receptor **1** with tetrafluorolinkers has higher binding constants for anions than receptor **2** (except for nitrate), showing the efficiency of the π-acidic surfaces' additivity within the confined space of our receptor. For halides, it can be observed that receptor **1** exhibits the strongest association constant with chloride (K_a = 207, Table 1, entry 1). The binding constant is better than those previously reported for BTI receptors and more than ten times higher compared to that for hemicryptophane **2**, presenting less π-acidic surfaces.[23,24] These observations are also supported by ^{19}F NMR (Fig. S20†) as well as ESI-MS (Fig. S41†). Bromide and iodide affinities are weaker (Table 1, entries 2 and 3), which demonstrate slight selectivity. As postulated, hemicryptophane **2** shows much lower affinities for halides, 5 to 17 times lower for bromide and iodide, respectively. Next, we investigated the linear guest triiodide (Table 1, entry 4). Hemicryptophane **2** has no affinity for this guest, while hemicryptophane **1** shows the highest affinity (K_a = 416) among the tested anions. The highest polarizability of I_3^- could lead to stronger London and anion–π interactions, which might account for these experimental results. Moreover, this is the first example of the recognition of triiodide by a BTI-based receptor. Finally, we set out to investigate trigonal planar anions that might better fit the geometry of our molecular cages. Nitrate was evaluated since it is known to have a good affinity for electron-deficient receptors.[29] However, the titrations show very low affinity for our hosts, with the best binding obtained for receptor **2** (K_a = 66, Table 1, entry 5). The complex between hemicryptophane **2** and NO_3^- was also observed by ESI-MS (Fig. S44†). It could be suggested that the lack of recognition ability of **1** toward the nitrate anion might be due to electronic repulsion between nitrate and the fluorine atoms on the xylylene linkers. Acetate was also tested, and again higher binding constants were observed for the most electron-deficient receptor **1** (K_a = 99) (Table 1, entry 6). Anion screening was continued with larger volume anions such as hexafluorophosphate, perrhenate, dihydrogenphosphate and picrate, but these showed low or no affinity for hemicryptophanes **1** and **2** (K_a = 22, 28, <1, <1 for **1**, respectively, Table 1, entries 7–10).

We then performed DFT geometry optimization for the complex between chloride and hemicryptophane **1**. It was observed that the anion is positioned close to the BTI surface with a short distance to the carbon of the benzene moiety (d = 2.82 Å), supporting functional anion–π interactions (Fig. 5).

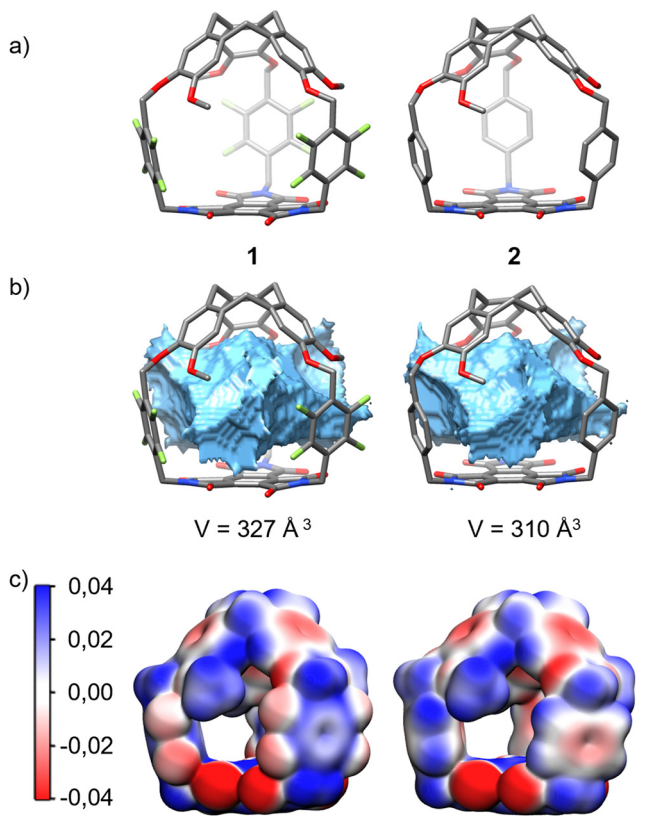

Fig. 4 (a) DFT optimized structure of hemicryptophanes **1** and **2**, together with their (b) calculated cavity volumes (MoloVol) and (c) electrostatic potential (ESP) maps. The ESP is mapped on the electron density iso-surface of 0.003 a.u. The red colour corresponds to a negative region of the electrostatic potential (–0.04 au), and the blue colour corresponds to the region where the potential is positive (+0.04 au).

Table 1 Binding constants of hemicryptophanes **1** and **2** for anions obtained by ^{1}H NMR titrations in $CDCl_3$ at 298 K (estimated error <20%)

Entry 1	Guest	1	2
1	Cl^-	207	20
2	Br^-	21	4
3	I^-	84	5
4	I_3^-	416	2
5	NO_3^-	<1	66
6	AcO^-	99	<1
7	PF_6^-	22	14
8	ReO_4^-	28	21
9	$H_2PO_4^-$	<1	<1
10	Picrate	<1	<1

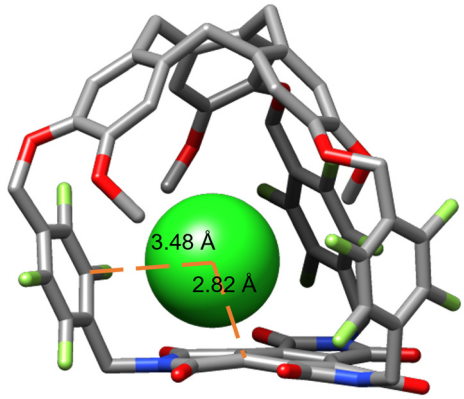

Fig. 5 Optimized structure of the complex Cl^-@hemicryptophane **1**.

Moreover, the electron-deficient perfluoroxylylene linker exposes its aromatic surface towards the chloride, which could increase anion recognition.

Conclusions

In conclusion, we have designed and synthesized an electron-deficient hemicryptophane receptor capable of effectively recognizing anions solely through enhanced anion–π interactions. By incorporating perfluoroxylylene arms and a benzene triimide (BTI) unit into the hemicryptophane structure, we created an electron-deficient confined environment that significantly improved anion affinity. Our binding studies revealed improved association constants for the hemicryptophane equipped with tetrafluoroxylylene linkers, particularly for chloride (K_a = 207), and a unique affinity for triiodide, representing the first instance of triiodide recognition by a BTI-based receptor. These results underscore the effectiveness of combining π-acidic surfaces within the receptor's cavity to strengthen binding affinities with anions. Moving forward, this strategy could be applied to develop more selective and efficient systems for complex biological and environmental applications where precise anion recognition is crucial.

Data availability

The data supporting this article have been included as part of the ESI.†

Conflicts of interest

There are no conflicts to declare.

Acknowledgements

Y. C. and A. M. thank the Agence Nationale de la Recherche for funding the APICOCAT project (grant ANR-21-CE07-0011) and the Co-LAB project (grant ANR-19-CE07-0024). We would like to thank Sabine Chevallier Michaud for low-resolution mass spectrometry and the Spectropole in Marseille for characterization. We also acknowledge the 'Centre de Calcul Intensif d'Aix-Marseille' for granting us access to its high-performance computing resources.

References

1 N. H. Evans and P. D. Beer, *Angew. Chem., Int. Ed.*, 2014, **53**, 11716.
2 H. Li, H. Valkenier, P. R. Brotherhood, S. Hussain, J. A. Cooper, O. Jurček, H. A. Sparkes, D. N. Sheppard and A. P. Davis, *Nat. Chem.*, 2016, **8**, 24.
3 P. Ballester, *Chem. Soc. Rev.*, 2010, **39**, 3810.
4 N. Busschaert, C. Caltagirone, W. Van Rossom and P. A. Gale, *Chem. Rev.*, 2015, **115**, 8038.
5 K. A. Jolliffe and P. A. Gale, *Org. Biomol. Chem.*, 2022, **20**, 713.
6 I. A. Rather, S. A. Wagay and R. Ali, *Coord. Chem. Rev.*, 2020, **415**, 213327.
7 Y. Zhao, Y. Cotelle, L. Liu, J. López-Andarias, A.-B. Bornhof, M. Akamatsu, N. Sakai and S. Matile, *Acc. Chem. Res.*, 2018, **51**, 2255.
8 A. Frontera, P. Gamez, M. Mascal, T. J. Mooibroek and J. Reedijk, *Angew. Chem., Int. Ed.*, 2011, **50**, 9564.
9 M. Giese, M. Albrecht and K. Rissanen, *Chem. Rev.*, 2015, **115**, 8867.
10 D.-X. Wang and M.-X. Wang, *Acc. Chem. Res.*, 2020, **53**, 1364.
11 J. Luo, J. Zhu, D.-H. Tuo, Q. Yuan, L. Wang, X.-B. Wang, Y.-F. Ao, Q.-Q. Wang and D.-X. Wang, *Chem. – Eur. J.*, 2019, **25**, 13275.
12 S.-Y. Zhuang, Y. Cheng, Q. Zhang, S. Tong and M.-X. Wang, *Angew. Chem., Int. Ed.*, 2020, **59**, 23716.
13 M.-D. Gu, Y. Lu and M.-X. Wang, *J. Org. Chem.*, 2020, **85**, 2312.
14 H.-B. Liu, Q. Zhang and M.-X. Wang, *Angew. Chem., Int. Ed.*, 2018, **57**, 6536.
15 D.-X. Wang, Q.-Q. Wang, Y. Han, Y. Wang, Z.-T. Huang and M.-X. Wang, *Chem. – Eur. J.*, 2010, **16**, 13053.
16 S. T. Schneebeli, M. Frasconi, Z. Liu, Y. Wu, D. M. Gardner, N. L. Strutt, C. Cheng, R. Carmieli, M. R. Wasielewski and J. F. Stoddart, *Angew. Chem., Int. Ed.*, 2013, **52**, 13100.
17 D. Quinonero, C. Garau, C. Rotger, A. Frontera, P. Ballester, A. Costa and P. M. Dey, *Angew. Chem., Int. Ed.*, 2002, **41**, 3389.
18 C. Garau, D. Quiñonero, A. Frontera, P. Ballester, A. Costa and P. M. Deyà, *J. Phys. Chem. A*, 2005, **109**, 9341.
19 D. Zhang, A. Martinez and J.-P. Dutasta, *Chem. Rev.*, 2017, **117**, 4900.
20 J. B. Carroll, M. Gray, K. A. McMenimen, D. G. Hamilton and V. M. Rotello, *Org. Lett.*, 2003, **5**, 3177.
21 K. A. McMenimen and D. G. Hamilton, *J. Am. Chem. Soc.*, 2001, **123**, 6453.
22 D.-H. Tuo, Q. He, Q.-Q. Wang, Y.-F. Ao and D.-X. Wang, *Chin. J. Chem.*, 2019, **37**, 684.

23 D.-H. Tuo, Y.-F. Ao, Q.-Q. Wang and D.-X. Wang, *Org. Lett.*, 2019, **21**, 7158.
24 D.-H. Tuo, Y.-F. Ao, Q.-Q. Wang and D.-X. Wang, *CCS Chem.*, 2021, **3**, 2876.
25 L. Miton, E. Antonetti, D. García-López, P. Nava, V. Robert, M. Albalat, N. Vanthuyne, A. Martinez and Y. Cotelle, *Chem. – Eur. J.*, 2024, **30**, e202303294.
26 J. Canceill, A. Collet, J. Gabard, G. Gottarelli and G. P. Spada, *J. Am. Chem. Soc.*, 1985, **107**, 1299.
27 M. Delecluse, C. Colomban, D. Moraleda, I. de Riggi, F. Duprat, S. Michaud-Chevallier, J.-P. Dutasta, V. Robert, B. Chatelet and A. Martinez, *Chem. – Eur. J.*, 2019, **25**, 3337.
28 D. B. Hibbert and P. Thordarson, *Chem. Commun.*, 2016, **52**, 12792.
29 L. Adriaenssens, C. Estarellas, A. Vargas Jentzsch, M. Martinez Belmonte, S. Matile and P. Ballester, *J. Am. Chem. Soc.*, 2013, **135**, 8324.